

A High-Fidelity Simulation Framework for Grasping Stability Analysis in Human Casualty Manipulation

Qianwen Zhao¹, Rajarshi Roy², Chad Spurlock², Kevin Lister², and Long Wang¹

Abstract—Recently, there has been a growing interest in rescue robots due to their vital role in addressing emergency scenarios and providing crucial support in challenging or hazardous situations where human intervention is difficult. However, very few of these robots are capable of actively engaging with humans and undertaking physical manipulation tasks. This limitation is largely attributed to the absence of tools that can realistically simulate physical interactions, especially the contact mechanisms between a robotic gripper and a human body. In this letter, we aim to address key limitations in current developments towards robotic casualty manipulation. Firstly, we present an integrative simulation framework for casualty manipulation. We adapt a finite element method (FEM) tool into the grasping and manipulation scenario, and the developed framework can provide accurate biomechanical reactions resulting from manipulation. Secondly, we conduct a detailed assessment of grasping stability during casualty grasping and manipulation simulations. To validate the necessity and superior performance of the proposed high-fidelity simulation framework, we conducted a qualitative and quantitative comparison of grasping stability analyses between the proposed framework and the state-of-the-art multi-body physics simulations. Through these efforts, we have taken the first step towards a feasible solution for robotic casualty manipulation.

I. INTRODUCTION

Rescue robots gain increasingly attention recently, in addressing emergency scenarios, providing critical support in situations where human intervention is challenging or hazardous. Most of literature in this field focus on the discovery and localization of victims, visual assessment of victims, and environmental information gathering [1–7]. Some of them put efforts on transporting victims through unstructured terrains [8–10]. Few of them considered active physical contacts with human, where [11–13] have demonstrate the ability in manipulating human body without considering biomechanical reactions of human body resulted from interactions with robots. Most recently, [14] investigated on generating biomechanically safe trajectories in search and rescue mission. However, all of the above examples have two limitations: (i) humans are simplified as a chain of rigid links connected by revolute joints; and (ii) the grasping problem (e.g. grab a body part) is ignored. These limitations have become roadblocks for advancing robotic casualty manipulation. As illustrated by the conceptual drawing in Fig. 1,



Fig. 1: The use of robotics and autonomous systems in search-and-rescue missions is a promising force-multiplier of military interests. Such robot systems need to ensure safe and effective grasping and manipulation of the wounded/incapacitated soldier.

the development of such casualty manipulation robot is still in its early stages. This is anticipated due to the high-risk nature of manipulating human bodies.

Research on human casualty manipulation remains a challenging task for various reasons. Firstly, investigations via experimental hardware with real human subjects present safety risks to human subjects. One common solution for this concern is to use simulation tools for rapid testing and iteration. However, a high-fidelity simulation tool is current absent. Such tool should be able to accurately simulate both the robot motion and the biomechanical reactions of human body. Secondly, ensuring grasping stability during casualty manipulation remains a significant concern. Grasping stability is a fundamental aspect for the successful execution of casualty manipulation tasks, as it directly impacts the safety and effectiveness of the robot’s actions.

In the current state-of-the-art (SotA), there exists research and literature focused on simulating human soft tissues for surgical applications. For example, [15] developed a soft liver model using FEM to support surgery planning and training, while [16] presented soft tissue models using FEM and studied their response to impulsive acoustic radiation force. More comprehensive models of human soft tissues for surgical applications can be found in survey papers [17], [18]. Additionally, research on grasping soft objects has also been undertaken [19], despite numerous studies on soft grippers [20–22]. However, the above are individual soft tissues rather than a comprehensive high-fidelity model of the entire human body. Therefore, none of the above has been utilized in solving casualty manipulation. The challenges of casualty manipulation remain. Within the context of casualty

¹Qianwen Zhao and Long Wang are with Charles V. Schaefer, Jr. School of Engineering and Science, Department of Mechanical Engineering, Stevens Institute of Technology, Hoboken, New Jersey, USA 07030 qzhao10, lwang4@stevens.edu

²Rajarshi Roy, Chad Spurlock, and Kevin Lister are with Corvid Technologies, Mooresville, NC, USA 28117 rajarshi.roy, chad.spurlock, kevin.lister@corvidtec.com

manipulation [1–14], humans are still simplified as a chain of rigid links, and the grasping problem is ignored.

In addressing the two critical limitations in human modeling and grasping problem for robot-assisted casualty manipulation, the contributions of this work are summarized below.

1. We developed a novel casualty manipulation simulation framework via utilizing a high-fidelity digital human model. The framework achieves accurate simulation of human biomechanical reactions resulting from robot manipulation actions.
2. Enabled by the developed framework, we investigated the grasping stability problem on casualty limbs. We provided qualitative and quantitative results using the proposed framework and compared them with state-of-the-art(SotA) casualty manipulation simulation methods. The discovery revealed limitations and unrealistics of the SotA casualty manipulation simulation methods.

To the best of our knowledge, we are the first to introduce FEM into the simulation pipeline for robotic manipulation of high-fidelity digital human models. The human models in this work consider muscle as passive elastic elements, and it has the potential to extend to have active muscle activation functions in the future. Furthermore, the analysis of grasping stability lays the foundation for successful execution of casualty manipulation tasks.

II. OUR PROPOSED SIMULATION FRAMEWORK

The proposed framework enables high-fidelity simulations of casualty manipulation via (i) introducing the FEM and a digital human model to the pipeline, and (ii) bridging the gap between physics-based multi-body dynamics simulators and finite-element (FE) solvers. The integration of these two types of simulators provides a comprehensive platform that combine the efficiency of the former in robot system kinematics computation and the high-fidelity soft contact mechanism of the latter. This synthesis opens the door to a wide range of applications, with a particular emphasis on scenarios involving robotic manipulation of human-like entities.

In conventional robotics simulations, tools like Gazebo and MuJoCo excel in representing rigid body interactions and are widely used for robot motion planning. However, a simulation that is robust does not mean it is realistic. They fall short when it comes to dealing with soft contacts and deformations, especially in scenarios involving human beings or soft objects. On the other side of the simulators’ spectrum, FE solvers, designed to handle continuous media, offer a more detailed representation of intra system behaviors. However, they struggle with the complexities of robot system kinematics due to the fact of breaking each robot component to individual nodes. Thereby, a complementary integration of the two fills each other’s gap. It enables high-fidelity simulations which require both precise robot grasping control and accurate modeling of contacts with deformable human bodies.

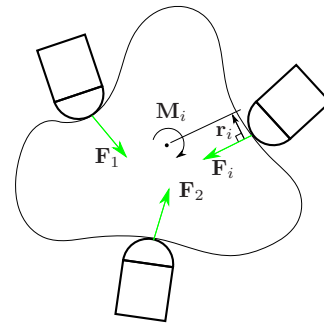


Fig. 2: Grasp static equilibrium for a rigid body.

Below, we discuss grasping equilibrium in both multi-body dynamics and FEM environments, respectively.

A. Equilibrium grasps in multi-body dynamics simulators

Simulations of grasping in multi-body dynamics simulators usually depend on rigid body mechanics, where both the robotic hand and the grasped object are modeled as rigid bodies. Consider an object grasped with N point contacts. All forces transmitted through the contacting bodies include normal forces and tangential forces due to friction, where all frictional forces lie strictly within their respective friction cones.

Shown in Fig. 2, the grasping equilibrium is governed by:

$$\sum_{i=1}^N \mathbf{F}_i + m\mathbf{g} = \mathbf{0}, \quad \sum_{i=1}^N (\mathbf{M}_i + \mathbf{r}_i \times \mathbf{F}_i) = \mathbf{0}, \quad \mathbf{F}_i, \mathbf{M}_i \in \mathbb{R}^3 \quad (1)$$

where $m\mathbf{g}$ represents gravity, and \mathbf{F}_i , \mathbf{M}_i , \mathbf{r}_i denote contact force, frictional moment, and moment arm, at the i^{th} contact, respectively.

Figure 7 (left) depicts the robotic hand grasping the human upper limb model at a predetermined location, establishing an equilibrium configuration where the arm object does not have translation or rotation.

B. Soft contacts equilibrium grasps using FEM

FEM is a numerical technique used in engineering and applied sciences for solving complex problems such as structural analysis, heat transfer, and fluid dynamics. In the

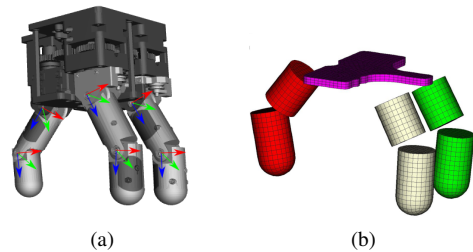


Fig. 3: Meshes of the custom robotic hand digits and the palm, (a) in a multi-body dynamics simulator; (b) in a FEM solver.

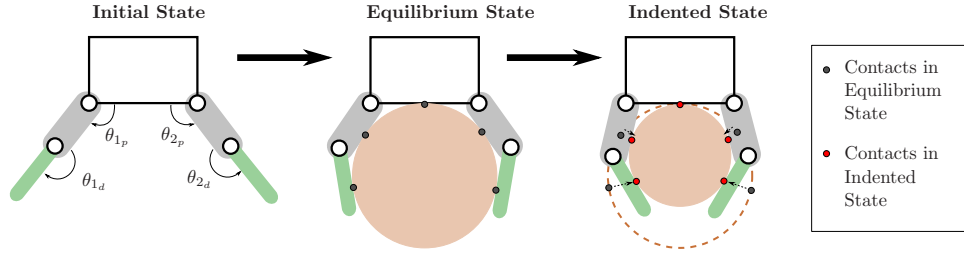


Fig. 4: Illustration of the state transitions among Initial State, Equilibrium State, and Indented State. Initial State is when the gripper is in its open position (left). Equilibrium State is when the grasping force equilibrium is reached (middle). Indented State is reached after each joint continuing to rotate further after the equilibrium grasping state.

field of robotics, the usage of FEM is under-explored. We proposed to use FEM for simulating complex contact mechanisms. FEM excels in handling complex geometries, material properties, and interactions within the system. These features make it particularly useful for simulating and analyzing contacts that involving soft materials (e.g. human body). Here are some key differences between physics-based multi-body dynamics simulators and FEM solvers, particularly in the application of robotics.

The first difference is in object representation, as illustrated in Fig. 3. In a multi-body dynamics simulator, the default representation is the rigid body transformation, including the origin position and frame orientation in the world frame. Figure 3(a) demonstrates frames rigidly attached to each robotic hand rigid links (finger segments). In a FE solver, on the contrary, shown in Fig.3(b), the same robotic hand are represented using numerous small elements composed of nodes. These elements within a single finger digit do not necessarily move together as a rigid group.

The second difference lies in motion descriptions as a result of the first difference. General motion of objects in a rigid-body dynamics simulator is measured with respect to their reference frame. In an FE engine, it is defined by motion of individual nodes on the geometry meshes.

The third difference is in simulation accuracy. FEM is known for its accuracy in representing detailed complex geometry with dissimilar materials. High fidelity surface deformation resulted from soft contacts can be computed using FEM with realistic material properties. In contrast, physics-based simulations may sacrifice accuracy for real-time performance. They are often used when real-time interactions and responsiveness are prioritized over detailed physical accuracy.

Figure 7 (right) shows the robotic hand grasping the high-fidelity digital human model in an FE solver, where human skin deformation is clearly visible.

C. The proposed integrative simulation framework

We propose a novel integrative framework to benefit from both environments: (1) computational convenience of rigid motion primitives in a multi-body dynamics simulator and (2) high fidelity of soft contact mechanics in an FE solver. The integration is achieved through three simulation states

illustrated in Fig. 4. From the *Initial State* to the *Equilibrium State* is accomplished through rigid environment grasping simulation, described in II-A. Moving from the grasping *Equilibrium State* to the *Indented State*, FEM (in II-B) enables the robotic hand to penetrate soft materials, resulting in realistic deformation and a soft contacts equilibrium grasp.

An illustrative example is presented in Fig. 5: a robotic hand squeezing a rubber sphere. Figure 5 (left) is the *Equilibrium State* with the rigid body assumption. Figure 5 (right) is the *Indented State*, where surface deformation is demonstrated and the heat map is overlaid to visualize the maximum principal strain. It can be seen that areas with greater deformation correspond to higher strain levels.

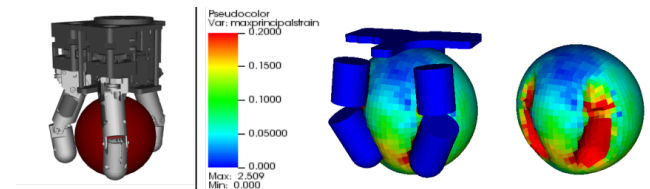


Fig. 5: An illustrative example of a simulation done in the proposed integrative framework. A robotic hand grasping at a rubber sphere. The left figure shows the *Equilibrium State*, and the right two figures show the *Indent State* with its maximum principal strain overlaid at surface.

III. GRASPING STABILITY ANALYSIS DURING CASUALTY MANIPULATION

Two case studies have been undertaken using the proposed integrative simulation framework. The objective is to thoroughly examine grasping stability and explore potential differences between simulations conducted in (i) a physics-based multi-body dynamics simulator and (ii) the proposed framework that integrate multi-body dynamics with FEM. Qualitative and quantitative comparisons are presented.

A gripper and a digital human model are used in all case studies in this work. The custom three-finger robotic hand in Fig. 3 serves as the gripper. The Computational Anthropomorphic Virtual Experiment Man (CAVEMAN) [23] model in Fig. 6 employed as the high-fidelity digital human model. It is developed by Corvid Technologies. It uses the detailed Zygote's 50th percentile male human CAD model

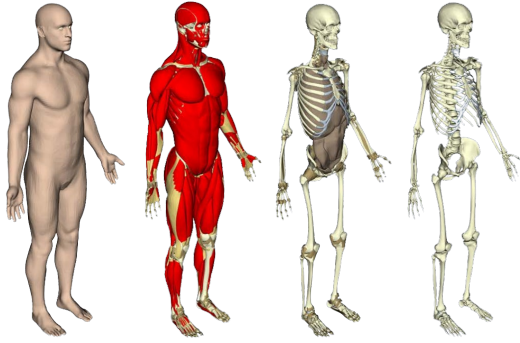


Fig. 6: The Computational Anthropomorphic Virtual Experiment Man (CAVEMAN) model, developed by Corvid Technologies.

[24] which includes representations of all components of the human musculoskeletal system. Material models utilized in the CAVEMAN model have been derived from literature and experimental tissue testing. The model connectivity matches all anatomical insertions as accurately as possible. The overall philosophy implemented during the creation of the CAVEMAN human body model focused on minimizing the use of simplifying assumptions to create an FE model which represents a cadaver as closely as possible.

A. Case studies: grasp and manipulation of human body

1) *Grasping at human upper limb*: The first case study aims to realistically simulate the act of grasping the human body at the upper limb, as depicted in Fig. 7. We chose the upper limb as it aligns with our natural perception of grabbing someone. Our focus is on assessing grasping stability, considering both rigid and soft simulation environments.

2) *Human upper limb manipulation*: In the second case study, which follows the first, we command the robotic hand to pull along the arm direction after establishing a stable grasp. Here, we concentrate on exploring the stability of grasping in the context of manipulating the human body, mimicking a pulling motion. Figure 8 illustrates the pulling of the CAVEMAN arm while maintaining the established grasp.

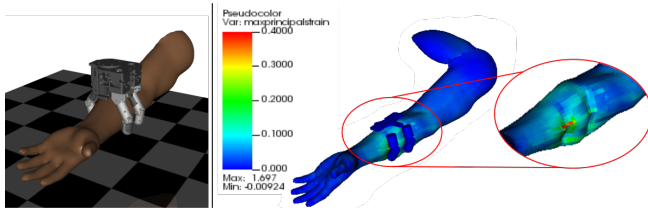


Fig. 7: Case study 1: Grasping at human upper limb. The left illustrates the simulation results in a multi-body dynamics simulator. The figure on the right demonstrates the results using the proposed simulation framework. The heat map depicts the maximum principal strain.

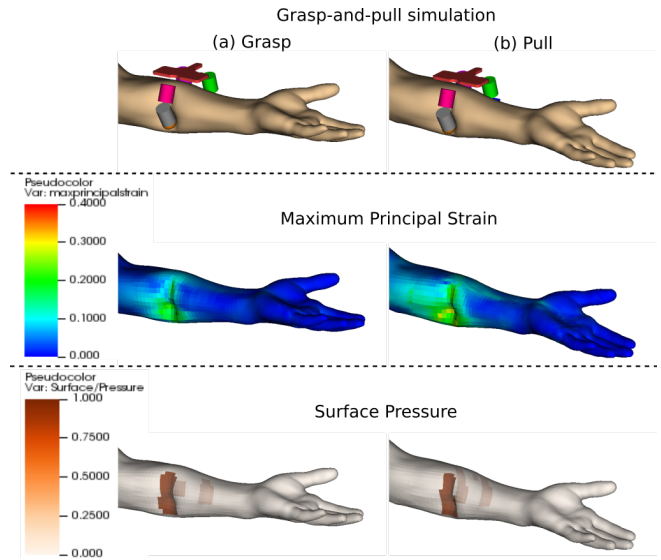


Fig. 8: Case Study 2: Grasp-and-pull simulation. Firstly, the robotic hand closes its palm to grasp the CAVEMAN arm, as shown in Case 1. Then, the robotic hand pulls along the CAVEMAN arm towards its wrist by 2cm. The three figures in column (a) depict the end of grasping, while the three figures in column (b) illustrate the end of pulling. All figures demonstrated simulation results in the proposed simulation framework.

B. Qualitative Comparison

Comparing simulation results between rigid (the multi-body dynamics simulator) and deformable environment (the proposed simulation framework) is visually straightforward. In the rigid setting, depicted in Fig. 7 (left), only several point contacts are established between the robotic hand and the human arm. Conversely, in the proposed simulation framework (deformable simulation environment) shown in Fig. 7 (right) and Fig. 8, realistic deformation can be observed in the human upper arm in the transition from the *equilibrium state* to the *indented state*. These deformations align with our expectations when grabbing someone's upper limb. Unlike in the rigid simulations, there is no penetration allowed even with aggressive force grasping on the human arm. The deformable environment permits more realistic results.

C. Quantitative Comparison of Grasping Stability

Grasping stability is crucial in casualty manipulation, serving as a prerequisite for all human body manipulation tasks. Whether focusing on safety, precision, comfort, or adaptability, achieving a stable grasp is always necessary to proceed effectively. However, obtaining high-fidelity simulation results isn't always feasible. This limits the transition of casualty manipulation robot systems from conceptualization to real-world application. In this section, we will evaluate grasping stability from two perspectives: (1) contact mechanisms, and (2) prevention of grasping slippage.

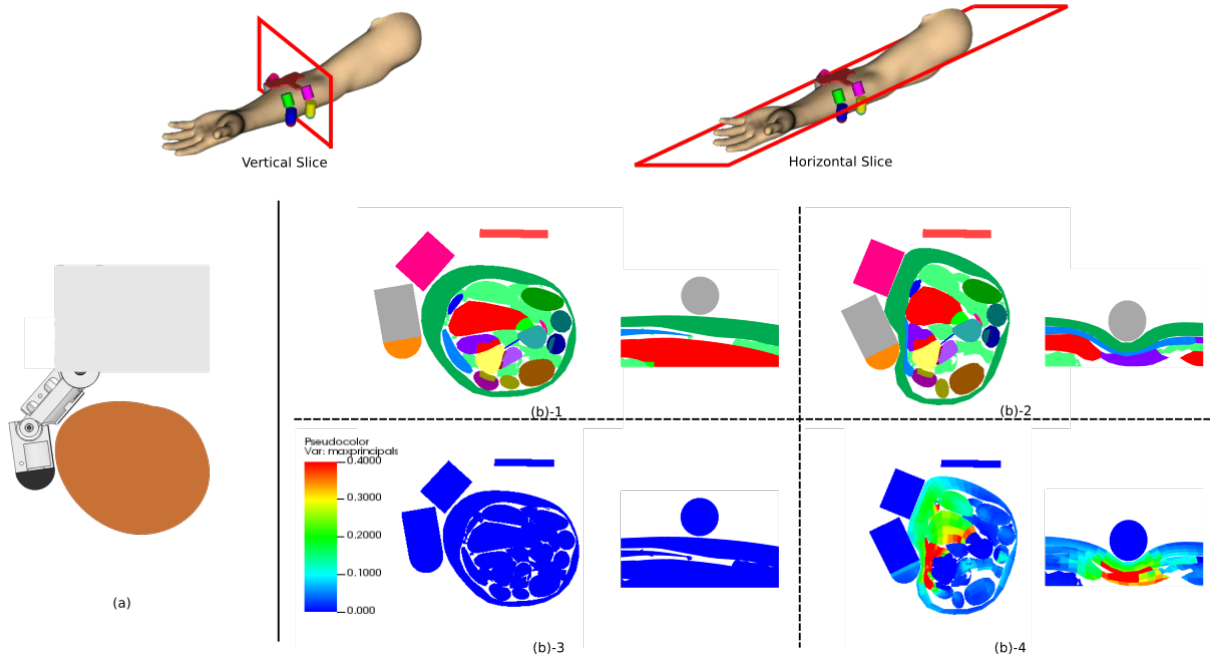


Fig. 9: Grasping simulations in two engines: (a) in a multi-body dynamics simulator, and (b) in proposed simulation framework. Sliced view are presented. (a) and (b)-left are sliced vertically, perpendicular to the human arm direction, as illustrated on the top left. It is referred as "vertically-sliced view" in the paper content. (b)-right are sliced horizontally, parallel to the robotic hand palm, as illustrated on the top right. It is referred as "horizontally-sliced view" in the paper content. (b)-1 and (b)-3 illustrate the *equilibrium state*, and (b)-2 and (b)-4 depict the *indented state*. Additionally, (b)-3 and (b)-4 are with the maximum principal strain heat map overlay.

Firstly, in comparing contact mechanisms in different simulation engines, the grasping simulation described in Case study 1 (III-A.1) is executed in both a multi-body dynamics simulator and the proposed simulation framework, respectively. Results can be seen in Fig. 9. In Fig. 9(a), it illustrates the 'vertically-sliced view' of simulation result of grasping at the digital human arm in the multi-body dynamics simulator. Here, the rigid body assumption is employed, and therefore, only point contacts are allowed. In Fig. 9(b), the same grasping simulation executed in the proposed simulation framework is shown, with a mix of 'vertically-sliced' and 'horizontally-sliced' view to clearly illustrate contacts. Figure. 9(b)-1 and (b)-3 are at the *equilibrium state* and (b)-2 and (b)-4 are in the *indented state*.

The comparison in contact mechanism is demonstrated, where the one with rigid body assumption has no deformation when contact happens. Conversely, the result from the proposed simulation framework shows human body muscle deformation. It is enabled by the integrated FE engine in the framework. Skin surface deformation data have also been abstracted and plotted in Fig. 10, where the node positions before and after grasping are shown in the same plot for comparison and visualization. Moreover, the interaction of body tissues resulting from the gripping motion is also demonstrated in Fig. 9(b)-3 and (b)-4 with the maximum principal strain heat map overlay. The maximum principal strain is generally proportional to the amount of deformation.

The results from the simulation in the FE engine realistically reflect the human body biomechanical response compared to that in the rigid simulation environment. Additionally, these results are invaluable for further safety evaluations and injury assessments.

Secondly, one of the most important criteria in assessing grasping stability is the ability to prevent slippage when

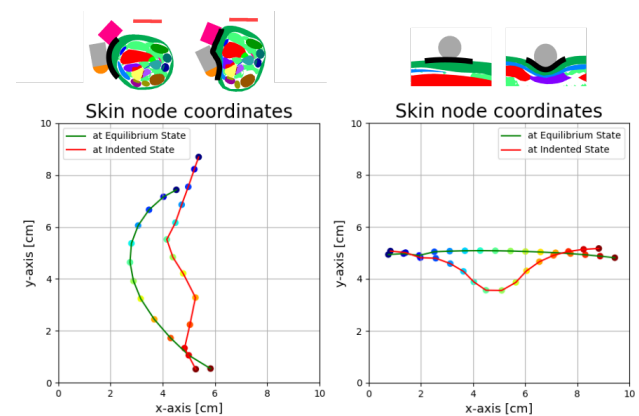


Fig. 10: CAVEMAN arm node positions before and after grasping are shown by green and red lines, respectively, with vertically (left) and horizontally (right) sliced views for intuitive illustration.

external disturbances are applied. For our specific application involving casualty manipulation tasks, we implemented grasp-and-pull simulations outlined in Case study 2 (III-A.2). These simulations are designed to assess grasping stability across various simulation engines, including the multi-body dynamics simulator used for the grasping simulations and the proposed simulation framework.

These two series of grasp-and-pull simulations involved defining 13 levels of grip tightness ranging from loose to tight. These levels were chosen to start from the *equilibrium state* and gradually increase the grip force until reaching the gripping force level of the *indented state*. At each level of grip tightness, we instructed the robotic hand to move along the CAVEMAN arm towards the wrist by 2cm while maintaining the grasp configuration. In the multi-body dynamics simulator, a one-dimensional slider is used to actuate the robotic hand, while in the proposed simulation framework, nodal displacement time history inputs are defined to achieve the same robotic hand pulling motion.

Simulation results need to be compared at a similar grip tightness level, to ensure the validity of the comparison. Grip tightness level was quantified by how tightly the fingers are closed around the CAVEMAN arm, meaning the normal contact force at each contact location. Given the grasping equilibrium condition, the normal contact force at each robotic hand finger should be at a similar level to preserve equilibrium. Therefore, we selected one of them, in our case, the thumb proximal link, to represent.

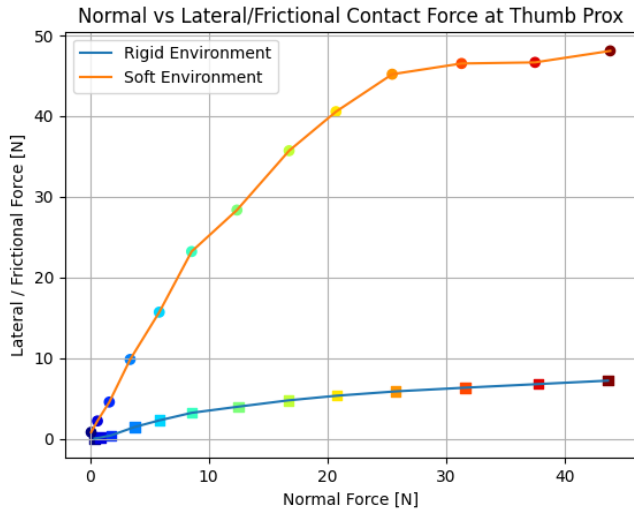


Fig. 11: Comparison of normal and lateral contact forces during the grasp-and-pull simulations. The blue line represents results from a multi-body dynamics simulator, while the orange line represents results from the proposed simulation framework. Data points on the lines are color-coded to indicate similar normal contact forces.

Figure 11 illustrates the results of two series of grasp-and-pull simulations. The focus is on comparing the contact normal force and lateral force. The blue line represents the contact information from the 13 multi-body dynamic

simulations. The orange line represents the contact data from the proposed high-fidelity simulation framework. Data points are color-coded to correspond to the 13 levels of grip tightness. All contact forces are projected to its local contact frame,

$$\mathbf{f}_n = (\hat{\mathbf{n}}_s \hat{\mathbf{n}}_s^\top) \mathbf{f} \quad (2)$$

$$\mathbf{f}_\mu = (\mathbf{I} - \hat{\mathbf{n}}_s \hat{\mathbf{n}}_s^\top) \mathbf{f} \quad (3)$$

where \mathbf{f} is the contact force vector, \mathbf{f}_n and \mathbf{f}_μ are the normal and tangential projections of \mathbf{f} , and $\hat{\mathbf{n}}_s$ is a unit vector that represents the normal direction of the contact surface, and \mathbf{I} is the identity matrix.

As observed from the blue line in Fig. 11, the frictional/normal force ratio is low and close to a linear relation. This is attributed to the rigid body point contact assumption. This assumption results in the contact mechanism that the contact force is more accurate in the normal direction. However, it does not effectively simulate the realism in preventing lateral motion, which leading to grasp slippage. Conversely, the contact profile from the proposed high-fidelity simulation framework behaves differently. A data point on the steeper line (orange line) in Fig. 11 indicates a grasp that offers better resistance to lateral motion. This indicates a more stable grasp. On the orange line, the lateral force is consistently greater than the normal contact force, regardless of the grip tightness level. This is because in proposed simulation framework, not only does frictional force contribute to the lateral force, but more importantly, the contact force at deformation prevents the CAVEMAN arm from slipping when disturbances are applied. Figure 12 illustrates the elastic deformation that prevents grasping slippage.

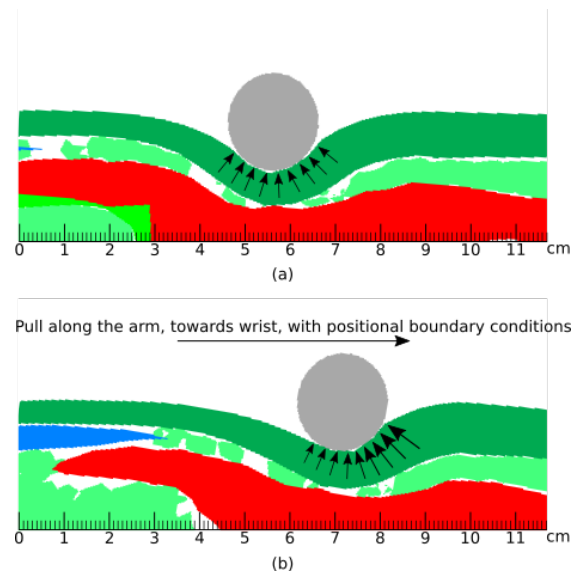


Fig. 12: Human body deformation and reaction force during the grasp-and-pull simulation in the FE solver. (a) depicts the result at the end of grasping, while (b) illustrates the state at the end of pulling.

The combination of FEM and the detailed construction of the CAVEMAN model in the proposed simulation framework enables the attainment of high-fidelity contact results. FEM effectively breaks down complex problems into smaller, more manageable elements interconnected by nodes. Each element is characterized by its material and geometric properties, facilitating accurate calculations of its behavior under diverse conditions. Notably, FEM excels in simulating and analyzing continuous media with a focus on internal interactions. Similarly, the intricate responses of under-skin body tissues to human-robot physical interactions can benefit from unique features of FEM. Human body tissues exhibit complex properties that vary with factors like locations, orientation, and strain rate [25]. The CAVEMAN model stands as a comprehensive representation of the human body, encompassing the full skeleton, 397 muscles, 342 ligaments, 16 organs, and skin. This extensive detail ensures an accurate representation of various biological tissues.

We apply the strength of FEM into simulating robotic grasping and manipulation tasks. We believe that only using multi-body dynamics simulators is insufficient for supporting casualty manipulation tasks. As discussed previously, the rigid point contact assumption make the simulation results large deviated from reality. Only limited material properties, such as friction, can be specified in a multi-body dynamics simulator. However, in the proposed simulation framework with FEM integration, material properties are highly customizable and can be defined very close to human being biological systems. As a result, this capability enables the representation of complex nonlinear biomechanical behaviors that occur during physical contact between humans and robots.

In summary, our study highlights a significant contribution by quantitatively revealing the biases and inaccuracies inherent in current SotA physics-based multi-body dynamics simulators when predicting grasping stability in casualty manipulation scenarios. For instance, as illustrated in Fig. 11, the multi-body dynamics simulator predicts a frictional drag force of less than 10N, even with a high grasping actuation force of 40N. While with the same level of grip tightness, the proposed high-fidelity simulation framework suggests a lateral drag force of almost 50N. The trend line of the proposed simulation framework has a linear region and reached a plateau at higher grip tightness levels; however, the non-realistic results received from the multi-body dynamics simulator has a linear trend line entirely. This substantial discrepancy arises due to the differing fidelity levels of the two tools, each with varying computational costs. It is crucial for robotic planners to be aware of these potential unrealistic predictions by SotA simulators. Future research may explore a more balanced solution between accuracy and computational cost.

D. Comparisons on Computation Time and Environments

When setting up simulations, the approaches and considerations differ between a multi-body dynamics simulator and the proposed framework. Multi-body dynamics simulators

focus on defining the rigid bodies and their interconnected joints or constraints, emphasizing motion and interaction over material properties. While material properties are not directly modeled, parameters such as friction coefficient and contact stiffness are defined for accurate interactions between the robotic hand and human model. Conversely, in the proposed high-fidelity simulation framework with FEM integrated, CAVEMAN and the robotic hand are discretized into small elements connected by nodes, allowing for a detailed representation of geometry and material properties. Specific materials must be defined for each human body parts and the robotic hand. In addition, boundary conditions and material properties need to be specified for each elements.

When comparing simulation time consumption and computational cost, multi-body dynamics simulators typically offer nearly real-time simulations and lower computational costs compared to proposed simulation framework. This is because the former focuses on rigid body motion and interaction. In contrast, the later requires longer time and higher computational cost due to fine meshing and the complex nature of FE models, especially for large-scale system such as a high-fidelity digital human model with nonlinear behavior. Each simulation of grasping at human upper limb, as shown in Fig. 7 needs over 10 hours to compute.

IV. DISCUSSION

The proposed high-fidelity simulation framework for casualty manipulation represents a novel and effective integration of physics-based multi-body dynamics simulators and FEM. We are not utilizing the mechanics and physics results from the physics-based multi-body dynamics simulator; rather, we are only leveraging its effectiveness in solving robot kinematics. Our study suggests that relying solely on the physics-based multi-body dynamics simulator may not be adequate for realistically simulating casualty manipulation, as demonstrated in the findings presented in III-A.2.

V. CONCLUSION

In conclusion, this paper has addressed critical limitations in the development of robot-assisted casualty manipulation by introducing a novel simulation framework and conducting comprehensive investigations on grasping stability. The integration of the FEM into the simulation pipeline has enabled accurate modeling of biomechanical reactions during robot manipulation actions, leveraging a high-fidelity digital human model. Through qualitative and quantitative comparisons across various simulation engines, the necessity and superior performance of the proposed framework have been validated. This work marks an important initial step toward realizing a feasible solution for robot casualty manipulation, laying a solid foundation for future advancement in this field.

To advance this work towards real-world applicability, several future research directions can be pursued. Firstly, while FEM shows promise, its computational demands are a concern, especially for field deployment where real-time or near real-time operation is crucial. Our future plans

include leveraging various machine learning techniques to train models capable of predicting human body biomechanical reactions during robot contact. This approach aims to accelerate the response time of the casualty manipulation robot system, bringing it closer to real-world deployment. Secondly, the risk of causing further injuries to wounded soldiers during grasping and manipulation actions is another significant obstacle that limit the rapid development and iteration of casualty manipulation robot systems. Leveraging our high-fidelity digital human model, we intend to investigate the correlation between robot actions and potential human body injuries, such as exceeding joint load limits and ligament tears. This exploration will guide the development of a biomechanically-informed, safer, and more effective casualty extraction robot systems.

ACKNOWLEDGMENTS

This material is based on work that was supported by the U.S. Army Medical Research and Materiel Command (USAMRDC), Telemedicine and Advanced Technology Research Center (TATRC) through the Small Business Innovation research (SBIR) Program under contract number W81XWH22P0030. The views, opinions and/or findings contained in this research/presentation/publication are those of the author(s)/company and do not necessarily reflect the views of the Department of Defense and should not be construed as an official DoD/Army position, policy or decision unless so designated by other documentation. No official endorsement should be made. Reference herein to any specific commercial products, process, or service by trade name, trademark, manufacturer, or otherwise, does not necessarily constitute or imply its endorsement, recommendation, or favoring by the U.S. Government.

REFERENCES

- [1] S. Bhatia, H. S. Dhillon, and N. Kumar, "Alive human body detection system using an autonomous mobile rescue robot," in *2011 Annual IEEE India Conference*, 2011, pp. 1–5.
- [2] F. Niroui, K. Zhang, Z. Kashino, and G. Nejat, "Deep reinforcement learning robot for search and rescue applications: Exploration in unknown cluttered environments," *IEEE Robotics and Automation Letters*, vol. 4, no. 2, pp. 610–617, 2019.
- [3] E. Lygouras, N. Santavas, A. Taitzoglou, K. Tarchanidis, A. Mitropoulos, and A. Gasteratos, "Unsupervised human detection with an embedded vision system on a fully autonomous uav for search and rescue operations," *Sensors*, vol. 19, no. 16, 2019. [Online]. Available: <https://www.mdpi.com/1424-8220/19/16/3542>
- [4] G. A. Cardona and J. M. Calderon, "Robot swarm navigation and victim detection using rendezvous consensus in search and rescue operations," *Applied Sciences*, vol. 9, no. 8, 2019. [Online]. Available: <https://www.mdpi.com/2076-3417/9/8/1702>
- [5] W. Deng, K. Huang, X. Chen, Z. Zhou, C. Shi, R. Guo, and H. Zhang, "Semantic rgb-d slam for rescue robot navigation," *IEEE Access*, vol. 8, pp. 221 320–221 329, 2020.
- [6] J. P. Queralt, J. Taipalmaa, B. Can Pullinen, V. K. Sarker, T. Nguyen Gia, H. Tenhunen, M. Gabbouj, J. Raitoharju, and T. West-erlund, "Collaborative multi-robot search and rescue: Planning, co-ordination, perception, and active vision," *IEEE Access*, vol. 8, pp. 191 617–191 643, 2020.
- [7] C. Cruz, G. Sánchez, A. Barrientos, and J. Cerro, "Autonomous thermal vision robotic system for victims recognition in search and rescue missions," *Sensors*, vol. 21, p. 7346, 11 2021.
- [8] "Valkyrie: A patient recovery robot," <https://www.sbir.gov/sbirsearch/detail/203536>, accessed: 2023-02-06.

- [9] "A robotic system for wounded patient extraction and evacuation from hostile environments," accessed: 2023-02-06.
- [10] R. M. S. Jacob Rosen, Black Hannaford, *Surgical Robotics: Systems Applications and Visions*. New York, USA: Springer, 2011, ch. 2, pp. 13–32.
- [11] "Bear," <https://robotsguide.com/robots/bear>, accessed: 2024-02-23.
- [12] Z. Sun, H. Yang, Y. Ma, X. Wang, Y. Mo, H. Li, and Z. Jiang, "Bit-dmr: A humanoid dual-arm mobile robot for complex rescue operations," *IEEE Robotics and Automation Letters*, vol. 7, no. 2, pp. 802–809, 2022.
- [13] M. Yim, T. Cragg, and S.-K. Hayat, "Towards small robot aided victim manipulation," in *2009 IEEE International Workshop on Safety, Security and Rescue Robotics (SSRR 2009)*, 2009, pp. 1–6.
- [14] E. Peiros, Z.-Y. Chiu, Y. Zhi, N. Shinde, and M. C. Yip, "Finding biomechanically safe trajectories for robot manipulation of the human body in a search and rescue scenario," in *2023 IEEE/RSJ International Conference on Intelligent Robots and Systems (IROS)*, 2023, pp. 167–173.
- [15] A. Idkaidek and J. Iwona, "Toward high-speed 3d nonlinear soft tissue deformation simulations using abaqus software," in *Journal of Robotic Surgery*, vol. 9, 2015, pp. 299–310.
- [16] M. Palmeri, A. Sharma, R. Bouchard, R. Nightingale, and K. Nightingale, "A finite-element method model of soft tissue response to impulsive acoustic radiation force," *IEEE Transactions on Ultrasonics, Ferroelectrics, and Frequency Control*, vol. 52, no. 10, pp. 1699–1712, 2005.
- [17] U. Meier, O. Lopez, C. Monserrat, M.-C. Juan, and M. Alcañiz Raya, "Real-time deformable models for surgery simulation: A survey," *Computer methods and programs in biomedicine*, vol. 77, pp. 183–97, 04 2005.
- [18] J. Zhang, Y. Zhong, and C. Gu, "Deformable models for surgical simulation: A survey," *IEEE Reviews in Biomedical Engineering*, vol. 11, pp. 143–164, 2019. [Online]. Available: <https://api.semanticscholar.org/CorpusID:50785173>
- [19] Z. Lazher, J. A. Corrales Ramon, L. Sabourin, B. C. BOUZGARROU, and Y. Mezouar, "Grasp planning pipeline for robust manipulation of 3d deformable objects with industrial robotic hand + arm systems," *Applied Sciences*, vol. 10, p. 8736, 12 2020.
- [20] J. Zhou, S. Chen, and Z. Wang, "A soft-robotic gripper with enhanced object adaptation and grasping reliability," *IEEE Robotics and Automation Letters*, vol. 2, no. 4, pp. 2287–2293, 2017.
- [21] L. He, Q. Lu, S.-A. Abad, N. Rojas, and T. Nanayakkara, "Soft fingertips with tactile sensing and active deformation for robust grasping of delicate objects," *IEEE Robotics and Automation Letters*, vol. 5, no. 2, pp. 2714–2721, 2020.
- [22] Q. Jiang and F. Xu, "Design and motion analysis of adjustable pneumatic soft manipulator for grasping objects," *IEEE Access*, vol. 8, pp. 191 920–191 929, 2020.
- [23] K. Butz, C. Spurlock, R. Roy, C. Bell, P. Barrett, A. Ward, X. Xiao, A. Shirley, C. Welch, and K. Lister, "Development of the caveman human body model: Validation of lower extremity sub-injurious response to vertical accelerative loading," *Stapp car crash journal*, vol. 61, pp. 175–209, 11 2017.
- [24] Zygote. Solid 3D male model, url = <https://www.zygote.com/cad-models/collections-products/solid-3d-male-collection>, urldate = 2022-10-05.
- [25] "Body tissues — seer training." [Online]. Available: https://training.seer.cancer.gov/anatomy/cells_tissues_membranes/tissues/